CHEMISTRY
A European Journal

www.chemeurj.org

Reprint

A Journal of
ChemPubSoc Europe
ACES
Asian Chemical Editorial Society
WILEY-VCH

ChemPubSoc Europe

DOI: 10.1002/chem.201700553

CHEMISTRY A European Journal Full Paper

Donor–Acceptor Systems |Hot Paper|

5-(Hetero)aryl-Substituted 9-Hydroxyphenalenones: Synthesis and Electronic Properties of Multifunctional Donor–Acceptor Conjugates

Lisa Bensch,[a] Irina Gruber,[b] Christoph Janiak,[b] and Thomas J. J. Müller*[a]

Dedicated to Prof. Dr. Herbert Mayr on the occasion of his 70th birthday

Abstract: 5-(Hetero)aryl-substituted 9-hydroxyphenalenones (9-HP) can be readily synthesized by Suzuki coupling of 5-bromo 9-HP with (hetero)aryl boronic acid (derivatives) without protection of the hydroxyl functionality in moderate to excellent yields (57–94%). A library of 5-(hetero)aryl substituted 9-HP with broad substituent variation was studied with respect to their electronic properties (absorption and emission spectroscopies and cyclic voltammetry) and their computed electronic structures. All compounds show reversible reductive potentials between −1230 and −1110 mV and the donor-substituted representatives possess irreversible oxidation potentials around 600 mV. Compounds with electron-rich donors even show reversible oxidation potentials. Especially the donor-substituted 9-HPs display emission bands between 466 and 567 nm with quite large Stokes shifts (up to 4100 cm^{-1}). TD-DFT calculations nicely reproduce the spectroscopic data and Hammett correlations underline a pronounced resonance substituent influence on the photophysical properties.

Introduction

In the past years efficient and effective synthetic strategies for accessing functional organic chromophores have considerably gained a general interest.[1] Among several functional structural motifs donor–acceptor conjugates have found broad application, for instance in organic photovoltaics,[2] photocatalysis,[3] and model systems for artificial photosynthesis.[4] These conjugates consist of electron-rich donors and electron-deficient acceptor moieties. Although methoxy- or diethylamino-phenyl groups are often employed as donor moieties, the electron richness can be considerably enhanced by donor units such as phenothiazines[2a,5] and triarylamines.[2b,6] Besides fullerenes, typical electron acceptors are for example cyanophenyl groups, rhodaninylidene derivatives,[2b,7] and 9-hydroxyphenalenone (9-HP). In particular, 9-HP is a unique electron acceptor due to its ability to form stable radical anions[8] as well as metal complexes.[9] This metal-coordinating, radical-forming acceptor was first synthesized in 1941 by Koelsch from cinnamic acid and 2-methoxynaphthalene under Friedel–Crafts conditions.[10] Ever since then, many different syntheses have been published.[11] In addition 9-HP functionalization was intensively studied, but predominantly the transformation of the hydroxyl group into an amino group was addressed,[8a,12] and intensive studies of stabilized radicals[8a] and numerous metal complexes performed in detail.[9b–e,13] Interestingly, some complexes can be employed as catalysts,[14] neutral radical conductors,[15] and a europium complex embedded in mesoporous silica shows pronounced daylight-excited luminescence.[9e] But, to the best of our knowledge, the functionalization in the 5-position of the 9-hydroxyphenalenone has remained quite rare with the exception of two reports.[9c,16] On one hand methyl and propyl derivatives of palladium and rhodium complexes were investigated[9c] and in the other publication a trifunctional 1,9-dithiophenalenylium salt was synthesized and its neutral radical was studied. An alkyl protected 5,5′,5″-(1,3,5-phenylene)tris[9-(2-ethylhexoxy)-1-oxophenalene] was obtained as an intermediate product.[16] To the best of our knowledge, the synthesis and systematic study of electronic and photophysical properties of donor-9-HP conjugates has never been explored. Herein, we report the straightforward access to a plethora of 5-(hetero)aryl substituted 9-HP and a comprehensive study of their electronic properties (absorption, emission, redox potentials) and their computed electronic structure.

[a] L. Bensch, Prof. Dr. T. J. J. Müller
Institut für Organische Chemie und Makromolekulare Chemie
Heinrich-Heine-Universität Düsseldorf
Universitätsstraße 1, 40225 Düsseldorf (Germany)
E-mail: ThomasJJ.Mueller@uni-duesseldorf.de

[b] Dipl.-Wirtchem. I. Gruber, Prof. Dr. C. Janiak
Institut für Anorganische Chemie und Strukturchemie I
Heinrich-Heine-Universität Düsseldorf
Universitätsstraße 1, 40225 Düsseldorf (Germany)

Supporting information and the ORCID identification number(s) for the author(s) of this article can be found under https://doi.org/10.1002/chem.201700553.

Results and Discussion

Synthesis and structure

We reasoned that conjugated 5-substituted 9-HP systems should efficiently be accessible by Suzuki coupling of 5-bromo-9-hydroxyphenalenone (**1**) and aryl boronic acids **2** without the necessity of protection of the hydroxyl group due to a strong intramolecular hydrogen bond[17] (Scheme 1).

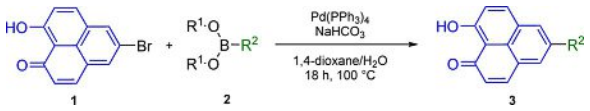

Scheme 1. Synthesis of 9-hydroxyphenalenone derivatives **3** by Suzuki coupling.

Therefore, we first set out to optimize the cross-coupling by a model reaction of 5-bromo 9-HP (**1**) and 4-methoxyphenyl boronic acid (**2a**) in a closed vessel at 100 °C for 18 h furnishing 5-(4-methoxyphenyl)-9-HP (**3a**) (Table 1). $Pd(PPh_3)_4$ (10 mol%) was selected as a suitable catalyst precursor and initially cesium carbonate was employed as a base in a THF/water mixture to give 52% of compound **3a** (Table 1, entry 1). Altering the base to sodium bicarbonate improved the yield of **3a** to 63% (Table 1, entry 2). Exchanging the co-solvent from water to methanol resulted in no improvement (Table 1, entry 3). Finally upon exchanging the co-solvent from THF to 1,4-dioxane a significant increase in yield to 81% was obtained (Table 1, entry 4).

Table 1. Optimization of the reaction conditions in the Suzuki coupling of 5-bromo-9-hydroxyphenalenone (**1**) with 4-methoxyphenyl boronic acid (**2a**).

Entry	Conditions Base	Solvent/co-solvent	Yield [%][a]
1	Cs_2CO_3	THF/H_2O	52
2	$NaHCO_3$	THF/H_2O	63
3	$NaHCO_3$	THF/MeOH	51
4	$NaHCO_3$	1,4-dioxane/H_2O	81

[a] The yield was determined by ^1H NMR with the external standard 1,3,5-trimethoxybenzene.

With these optimized conditions in hand we were able to exemplify the scope of this synthetic strategy by 14 different derivatives in moderate to excellent yields (Scheme 2). Electron-donating (e.g. **3a**) and -withdrawing groups (e.g. **3d**) in the aryl boronic acids and esters could be successfully employed in the reaction sequence, as well as heterocyclic substituents, such as isoquinoline (**3h**), thiophenes (**3k–n**) and pyrazoles (**3i,j**).

The structures of all conjugated 5-substituted 9-HP systems **3** were unambiguously assigned by ^1H and ^{13}C NMR spectroscopy, mass spectrometry, and they were additionally corroborated by X-ray crystal structure analyses of the compounds **3a** and **3i**. Compound **3a** crystallizes as needles (monoclinic space group $P2_1/c$). The 5-anisyl moiety is twisted out of copla-

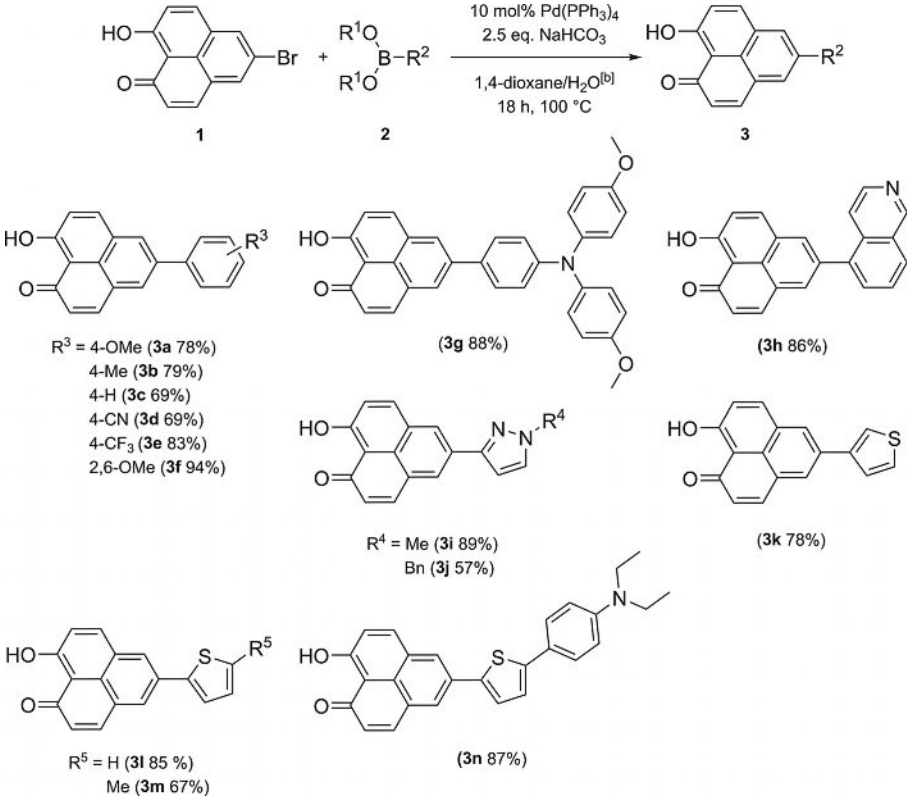

Scheme 2. Optimized reaction conditions (c(**1**) = 0.125 M) and synthesized examples of the Suzuki coupling with the isolated yield (after recrystallization).

narity with the 9-hydroxyphenalenone fragment by a dihedral angle of 47° (Figure 1). The phenol *H* atom is part of an intramolecular hydrogen bond to the quinone C=O atom (Figure 1).

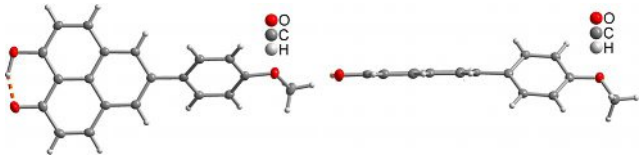

Figure 1. Molecular structure of **3a** (50% thermal ellipsoids), showing the intramolecular O–H···O bond as dashed orange line. H-bonding details O–H 1.06(3) Å, H···O 1.51(3) Å, O···O 2.508(2), O–H···O 153(2)°. The angle of 47° is the dihedral angle between the plane defined by the carbon atoms of the 9-hydroxyphenalenone fragment and the 5-anisyl moiety (See Supporting Information Figure S1 for graphic with atom numbering; details of bond lengths and angles are given in section 7.1 in the Supporting Information).

The molecules are stacked directly on top of each other with sizeable π–π stacking[18] along the *a*-direction and arranged in undulated layers parallel to the *bc*-plane. Besides the π-stacking interactions the intermolecular packing is organized by C–H···O hydrogen bonds (Figure 2).

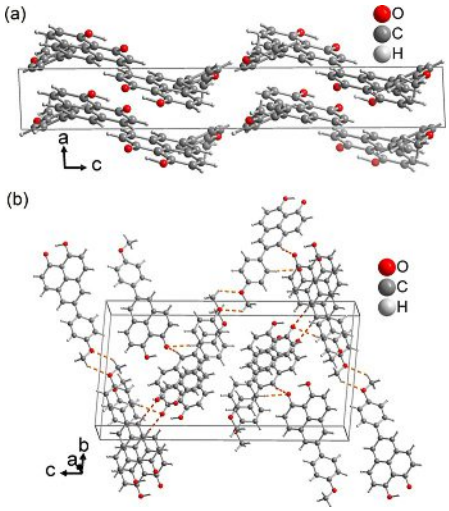

Figure 2. Sections of the packing diagram of **3a** showing the (a) undulated arrangement parallel to the *bc*-plane and (b) selected C–H···O interactions as orange dashed lines (For detailed information π-stacking and C–H···O interactions see section 7.1 in the Supporting Information).

Compound **3i** crystallizes as needles (orthorhombic space group $Pna2_1$). Both moieties, pyrazole and 9-HP, are arranged in a nearly coplanar orientation with a dihedral angle of 5° (Figure 3). The phenol H atom is part of an intramolecular hydrogen bond to the quinone C=O atom (Figure 4).

The molecules are stacked with sizeable π–π stacking (Figure S4a)[18] along the *c*-direction and are arranged in a herringbone pattern along the *a*-direction (Figure 4a). Along *b* the intermolecular packing is organized by C–H···N and C–H···O hydrogen bonds (Figure 4b). Interestingly, compound **3i** crystallizes in a non-centrosymmetric polar space group. This can be

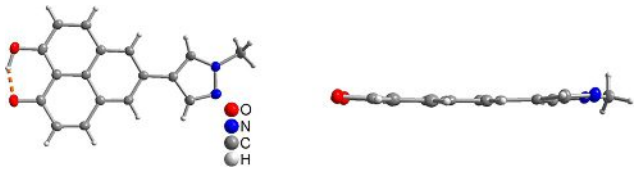

Figure 3. Molecular structure of **3i** (50% thermal ellipsoids), showing the intramolecular O–H···O bond as dashed orange line. H-bonding details O-H 1.02(4) Å, H···O 1.55(4) Å, O···O 2.504(2), O–H···O 152(3)°. The angle of 5° is the dihedral angle between the plane defined by the carbon atoms of the 9-hydroxyphenalenone fragment and the pyrazolyl moiety (See Supporting Information Figure S3 for graphic with atom numbering; details of bond lengths and angles are given in section 7.2 in the Supporting Information).

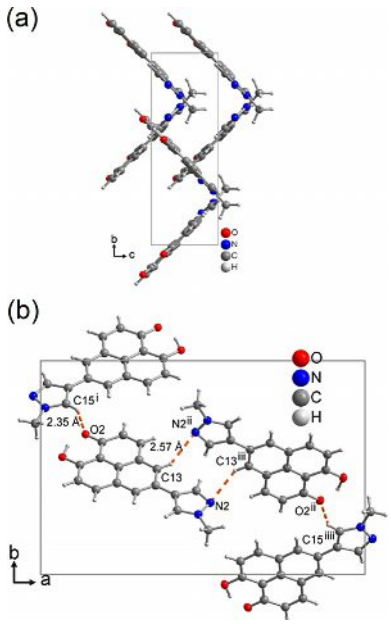

Figure 4. Sections of the packing diagram of **3i** showing (a) the herringbone arrangement along the *a*-axis and (b) selected C–H···N and C–H···O interactions as orange dashed lines. Symmetry transformations i = −1/2−*x*, −1/2+*y*, 3/2+*z*; ii = 1−*x*, 1−*y*, −1/2+*z*.

traced to the orientation of the molecules with the pyrazolyl end along the positive *c*-axis (Figure 4a).

Electrochemical properties

For determining the electrochemical properties cyclovoltammetric experiments were performed with all 5-(hetero)arylsubstituted 9-HP derivatives **3**. All compounds **3** possess Nernstian reversible reduction potentials $E_0^{0/-1}$ arising from the 9-HP part in a narrow range between −1110 and −1230 mV with exception of compound **3g** (Figure 5). The reduction potential of the 9-HP substituent is only affected to a minor extent by the remote substituents, yet the cathodic shift for electron releasing substituents and the anodic shift for electron withdrawing moieties can be clearly identified.

In the case of donor-9-HP systems, such as **3a** and **3g**, an additional irreversible oxidation potential $E_0^{0/+1}$ around 1400 mV can be detected. For compounds **3k** and **3l** the oxi-

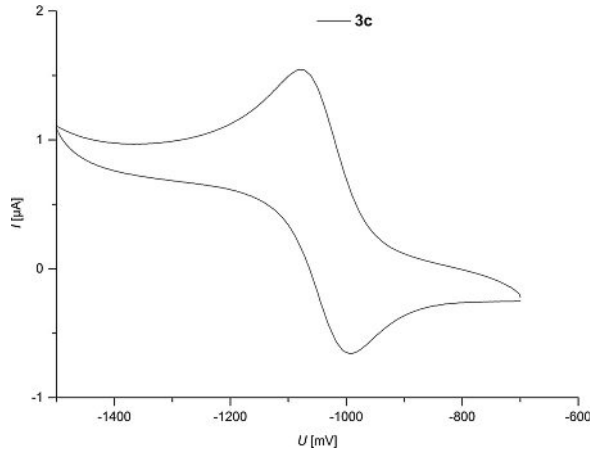

Figure 5. Cyclovoltammogram of compound **3c**, recorded in dichloromethane $T = 293$ K, electrolyte: $[Bu_4N][PF_6]$, Pt working electrode, Pt counter electrode, Ag/AgCl reference electrode.

dation events fall too close to the margin of the measuring window, and they were therefore neglected.

Compounds **3g** and **3n** behave slightly differently. By virtue of the powerful 4-(bis(4-methoxyphenyl)amino substituent in compound **3g** no reduction potential can be found. However, a unique Nernstian reversible oxidation potential $E_0^{0/+1}$ at 620 mV and an irreversible oxidation potential $E_0^{+1/+2}$ at 1330 mV can be determined. Compound **3n** is conjugatively ligated by thiophene with a strong aniline donor. This particularly electron rich system results in two reversible oxidation potentials ($E_0^{0/+1} = 650$ mV and $E_0^{+1/+2} = 1170$ mV) and an irreversible oxidation wave $E_0^{+2/+3}$ at 1720 mV (Table 2).

Hammett correlation

The reduction potentials of compounds **3a**–**3e** were correlated with Hammett parameters for scrutinizing the influence of polar substituents in *para*-position of aryl rings (Table 3). The influence of the substituent is best reflected by a correlation with σ_p (σ_p: $R^2 = 0.863$; σ_I: $R^2 = 0.522$; σ_R: $R^2 = 0.611$), which accounts for both the inductive sigma constant σ_I and the resonance sigma constant σ_R ($\sigma_p = \sigma_I + \sigma_R$).[19] This can be interpreted that the remote substituent operates by both resonance and inductive mechanisms (Figure 6). The overall variation of the reductive potential within a margin of 60 mV is, however, quite small.

Table 2. Selected electronic properties of the 9-hydroxyphenalenone derivatives **3**.[a]

Structure	$E_0^{0/-1}$	$E_0^{0/+1}$	$E_0^{+1/+2}$	$E_0^{+2/+3}$
3a	−1170	1530[b]	–	–
3b	−1170	–	–	–
3c	−1150	–	–	–
3d	−1140	–	–	–
3e	−1110	–	–	–
3f	−1230	–	–	–
3g	–	620	1330[b]	–
3h	−1140	–	–	–
3i	−1150	1490[b]	–	–
3j	−1130	1550[b]	–	–
3k	−1140	–[c]	–	–
3l	−1120	–[c]	–	–
3m	−1170	1360[b]	–	–
3n	−1160	650	1170	1720[b]

[a] Recorded in dichloromethane, $T = 293$ K, electrolyte: $[Bu_4N][PF_6]$, Pt working electrode, Pt counter electrode, Ag/AgCl reference electrode, $E_0 = (E_{pa} + E_{pc})/2$ with $[Fc]/[Fc]^+$ or $[Me_{10}Fc]/[Me_{10}Fc]^+$ as a standard. [b] Irreversible maximum. [c] The irreversible maximum is at the edge of the measurement range.

Table 3. Reduction potentials of the compounds **3a**–**3e** and the substituents corresponding Hammett parameter.

	$E_0^{0/-1}$	σ_R[20]	σ_p[20]
R^1 = 4-OMe **3a**	−1170	−0.56	−0.27
R^1 = 4-Me **3b**	−1170	−0.18	−0.17
R^1 = 4-H **3c**	−1150	0	0
R^1 = 4-CF_3 **3d**	−1140	0.15	0.54
R^1 = 4-CN **3e**	−1110	0.16	0.66

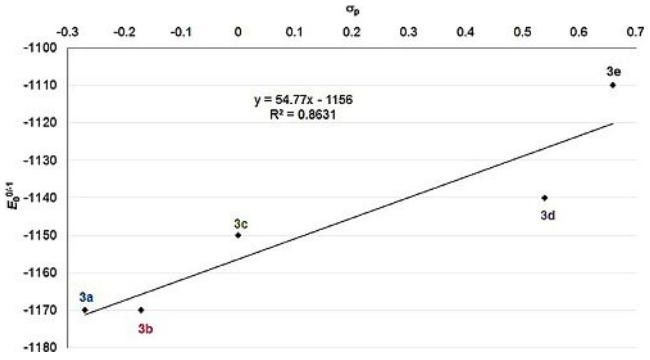

Figure 6. Hammett correlation between the reduction potential and σ_p of the compounds **3a**–**3e**.

Photophysical properties

All conjugated 5-substituted 9-HP systems **3** are yellow to red compounds and most of them show fluorescence in solution upon irradiation with UV light. Therefore, the photophysical properties were investigated by UV/Vis and static fluorescence spectroscopy.

Figure 7 shows the normalized absorption and emission spectra of the compounds **3a**–**3f** measured in acetonitrile. The bathochromic shift of the longest wavelength absorption maximum and the emission maximum with increasing donor character of the remote substituent R^1 is clear. The other two maxima at shorter wavelengths are almost not affected by this substituent.

All compounds show three distinct absorption maxima. The shortest wavelength absorption maxima appear between 268–302 nm with highest extinction coefficients ε ($\varepsilon \geq 17400\ L\,mol^{-1}\,cm^{-1}$). The second absorption maxima are located between 305 and 378 nm. Whereas for some compounds (**3e**, **3g**, and **3j**) the maximum clearly consists of two transitions others (**3a**, **3k**, and **3i**) only display shoulders close to

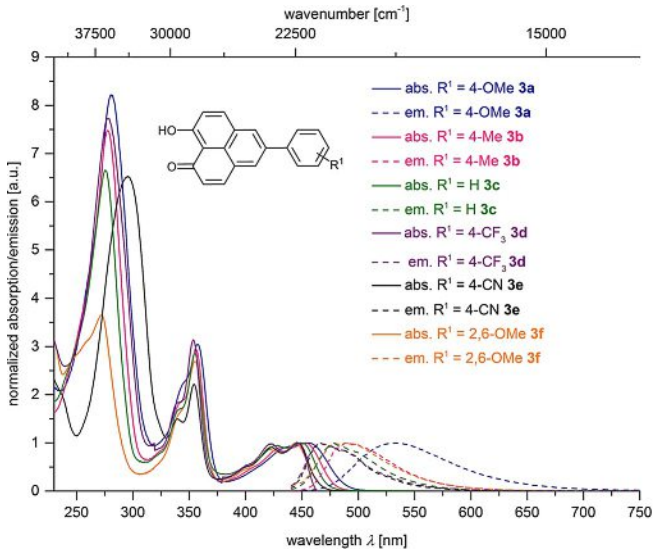

Figure 7. Selected normalized absorption (bold lines) and emission (dashed lines) spectra of 9-hydroxyphenalenone derivatives **3a**–**3f**, recorded in MeCN at $T = 298$ K ($c(\mathbf{3}) = 10^{-5}$ M). Emission spectra were recorded with $\lambda_{ex} = 420$ nm ($c(\mathbf{3}) = 10^{-7}$ M, standard for Φ_f: Coumarin 153 in MeOH, $\lambda_{ex} = 420$ nm).

the maxima. This absorption band has the second highest extinction coefficient, which lies between 9400–19200 L mol^{-1} cm^{-1}. The longest wavelength absorption maximum is between 421 and 486 nm—also this one can be found split into two peaks or just appear as one with a shoulder (Table 4)—with extinction coefficients between 2600–7500 L mol^{-1} cm^{-1}. This longest wavelength absorption maximum depends on the compound and its electronic structure, so donor moieties have a larger bathochromic shift (e.g. **3a** and **3m**) than acceptor substituted derivatives (e.g. **3d** and **3e**).

Table 4. Selected UV/Vis absorption and emission data of the 9-hydroxyphenalenone derivatives **3a**–**3m**.

Cmpd.	$\lambda_{max,abs}$ [nm] (ε [L mol^{-1} cm^{-1}])[a]	$\lambda_{max,em}$ [nm] (Φ_f)[b]	Stokes shift $\Delta\tilde{\nu}$ [cm^{-1}][c]
3a	456 (5400)	533 (0.19)	3200
3b	453 (6500)	490 (0.06)	1700
3c	427 (6400), 450 (6800)	478 (0.05)	1300
3d	423 (5200), 445 (5300)	466 (0.03)	1000
3e	423 (6800), 446 (7500)	466 (0.03)	1000
3f	422 (6200), 455 (7100)	484 (0.05)	1800
3g	470 (2600)	–	–
3h	421 (6400), 444 (7000)	476 (0.05)	1500
3i	464 (5600)	520 (0.23)	2300
3j	462 (4700)	516 (0.24)	2300
3k	454 (4000)	533 (0.09)	3300
3l	457 (5900)	500 (0.25)	1900
3m	461 (4300)	567 (0.32)	4100
3n	486 (3700)	513 (0.05)	1100

[a] Recorded in acetonitrile, $T = 293$ K, $c(\mathbf{3}) = 10^{-5}$ M. [b] Recorded in acetonitrile, $T = 293$ K, $c(\mathbf{3}) = 10^{-7}$ M, fluorescence quantum yield were determined relative to coumarin 153 in MeOH ($\Phi_f = 0.45$),[21] $\lambda_{ex} = 420$ nm. [c] $\Delta\tilde{\nu} = \lambda_{max,abs} - \lambda_{max,em}$ [cm^{-1}].

The emission maximum, which is found between 466 and 567 nm shows the same shift with quite high Stokes shifts. Compound **3m** displays the largest Stokes shift with 4100 cm^{-1} ($\lambda_{max,em} = 567$ nm), although all other Stokes shifts are usually around 2000 cm^{-1}. Only compound **3g** is essentially nonluminescent, presumably since the aryl rings are twisted out of coplanarity. The fluorescence quantum yields of the 9-hydroxyphenalenone derivatives **3** are highest for the 4-methoxyphenyl, thiophene and pyrazole derivatives. They were determined relative to coumarin 153 in methanol.

The bathochromic shift with increasing the donor character in the fluorescence is shown in Figure 8. The emission color is shifted from blue via yellow to orange.

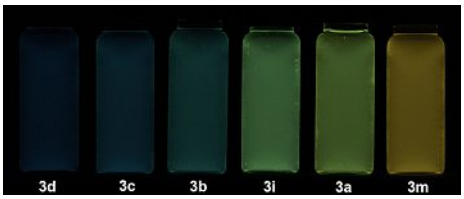

Figure 8. Fluorescence of selected 9-hydroxyphenalenone derivatives **3** in acetonitrile ($c(\mathbf{3}) = 10^{-5}$ M, hand-held UV-Lamp, $\lambda_{ex} = 365$ nm).

In addition the base-induced halochromicity of the UV/Vis absorptions of compound **3a** was studied. Tetrabutylammonium hydroxide·30 H_2O was chosen as a suitable base to deprotonate compound **3a**.[22] The pH-value was successively increased from pH 7.00 to 9.19 and the corresponding UV spectra were recorded. Upon deprotonation a redshift of all absorption bands can be detected (Figure 9) and the pK_a was determined to 8.91. In comparison to phenol (p$K_a = 9.95$ in H_2O)[23] compound **3a** is slightly more acidic. The influence of the substituents (donor and acceptor) on the pK_a value is only marginal, that is, within a range of 0.1 pK units.

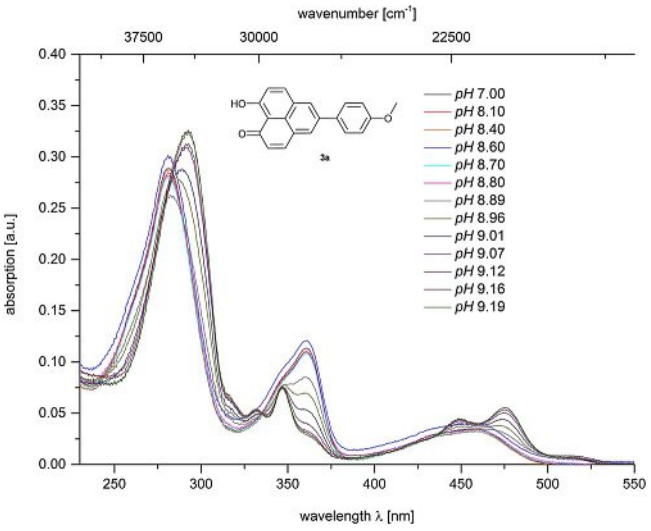

Figure 9. Absorption spectra of **3a** with successive addition of tetrabutylammonium hydroxide 30 H_2O, recorded in MeCN:H_2O (1:1) at $T = 298$ K ($c(\mathbf{3}) = 10^{-6}$ M).

Computational studies

The ground state geometry of compound **3a** was optimized by DFT calculations using the program package Gaussian09 with the B3LYP functional[24] and the Pople 6–31+G* basis set.[25] The polarizable continuum model (PCM) with acetonitrile as a solvent was implemented for later addressing the absorption and emission characteristics in solution.[26] All energy minimum structures were unambiguously confirmed by analytical frequency analysis. The calculated ground state structure of **3a** is shown in Figure 7. The torsional angle between the 9-hydroxyphenalenone and benzene moieties in solution is 38° and in good agreement with the crystal structure ($\theta = 45°$) (Figure 10).

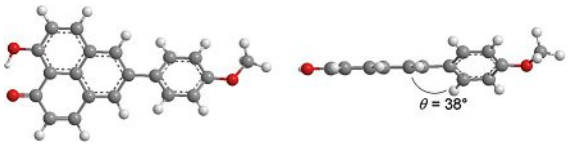

Figure 10. Optimized ground state and torsions angle θ of 9-hydroxy-5-(4-methoxyphenyl)-1*H*-phenalen-1-one **3a** obtained by application of the polarizable continuum model (PCM) with acetonitrile as solvent (Gaussian 09 B3LYP/6–31+G*).

The first five excited states were calculated on the TD-DFT level of theory by employing Gaussian09 with the B3LYP functional,[24] the Pople 6–31+G* basis set[25] and the polarizable continuum model (PCM) with acetonitrile[26] as a solvent for rationalizing the absorption characteristics. The experimental UV/Vis absorption maxima are nicely reproduced by the calculated data and allow the assignment of the optical transitions in the absorption spectra (Table 5). Two of the calculated maxima are found in the experimental spectra as shoulders and they are therefore only given as a range. The most dominant contribution in the longest wavelength absorption band of arises from the HOMO–LUMO transition (excited state 1). All other states consist of two or three FMO transitions (excited states 2–5).

The calculated maximum of the fluorescence using Gaussian09 with the B3LYP functional,[24] the Pople 6–31+G* basis set[25] and the polarizable continuum model (PCM) with acetonitrile as a solvent[26] is 556 nm. This is in reasonable agreement with the experimentally determined value of 533 nm. For its calculation only the S_1 state was considered according to Kasha's rule.

As can be seen from the Kohn–Sham frontier molecular orbitals (HOMO and LUMO) in Figure 11 the coefficient density is distributed in the HOMO over the complete molecular framework. The coefficient density in the LUMO in comparison is exclusively localized in the 9-hydroxyphenalenone acceptor part of the computed model compound **3a**. All this indicates a rather moderate charge transfer character of the first excited state.

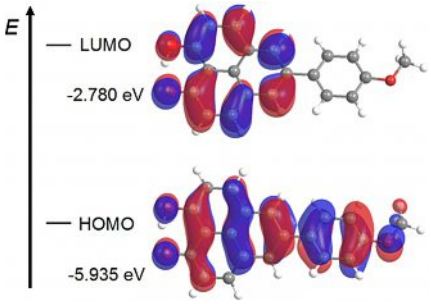

Figure 11. Selected Kohn–Sham frontier molecular orbitals of compound **3a** using the polarizable continuum model (PCM) with acetonitrile as solvent (Gaussian 09 B3LYP/6–31+G*).

Hammett correlation

The absorption and emission maxima and the Stokes shifts of the compounds **3a**–**3e** were correlated with Hammett parameters, which should confirm the influence of the substituent in *para*-position of the benzene ring (Table 6).[19]

The correlation of the resonance sigma parameter σ_R with the absorption and emission maxima gave best regression coefficients with $R^2 = 0.924$ for the absorption and $R^2 = 0.993$ for the emission (Figure 12).

The correlation with the other substituent Hammett parameters gave lower regression coefficients (absorption: σ_p: $R^2 = 0.892$, σ_p $R^2 = 0.262$; emission: σ_p: $R^2 = 0.682$, σ_I: $R^2 = 0.059$).

Table 5. TD-DFT calculated absorption maxima under specification of the most dominant contributions of compound **3a** using the polarizable continuum model (PCM) with acetonitrile as solvent (Gaussian 09 B3LYP/6–31+G*).

Excited state	$\lambda_{max,abs}$ calcd. [nm]	$\lambda_{max,abs}$ exp. [nm]	Oscillator strength	Dominant contributions	
1	463	456	0.052	HOMO→LUMO	98%
2	356	358	0.185	HOMO−1→LUMO	87%
				HOMO−2→LUMO	7%
3	334	335–346[a]	0.160	HOMO−2→LUMO	82%
				HOMO−1→LUMO	6%
				HOMO→LUMO+1	4%
4	284	280	0.999	HOMO→LUMO+1	92%
				HOMO−2→LUMO	3%
5	269	255–270[a]	0.182	HOMO→LUMO+2	77%
				HOMO→LUMO+3	14%
				HOMO−3→LUMO+1	2%

[a] Shoulder of the next absorption maximum.

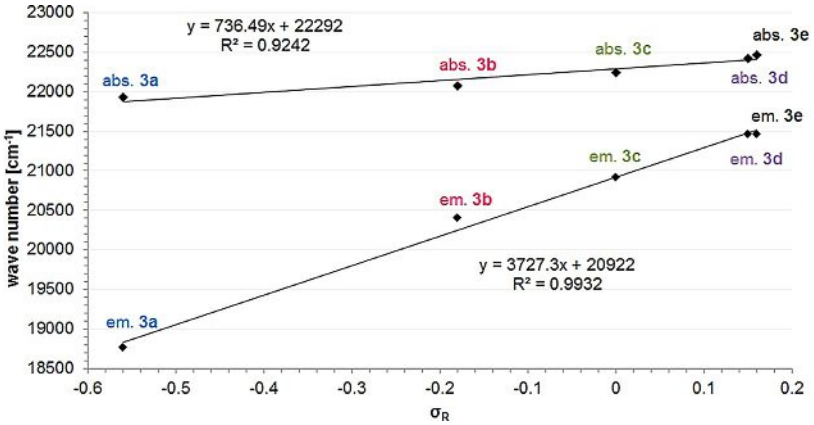

Figure 12. Hammett correlation between the absorption (abs.) and emission (em.) maxima and the resonance sigma parameter σ_R of the compounds **3a**–**3e**.

Table 6. Absorption and emission maxima and reduction potentials of the compounds **3a**–**3e** and the substituents corresponding Hammett parameter.

	$\tilde{\nu}_{max,abs}$ [cm^{-1}]	$\tilde{\nu}_{max,em}$ [cm^{-1}]	Stokes shift $\Delta\tilde{\nu}$ [cm^{-1}]	$\sigma_R^{[20]}$	$\sigma_p^{[20]}$
R^1 = 4-OMe **3a**	21900	18800	3200	−0.56	−0.27
R^1 = 4-Me **3b**	22100	20400	1700	−0.18	−0.17
R^1 = 4-H **3c**	22200	20900	1300	0	0
R^1 = 4-CF_3 **3d**	22500	21500	1000	0.15	0.54
R^1 = 4-CN **3e**	22400	21500	1000	0.16	0.66

This underlines that the absorption and emission strongly depends on the resonance effect and not on the inductive effect, but the excited state experiences a stronger influence by donor substituents compared to the ground state. Expectedly, the Stokes shifts also correlate nicely with the resonance parameter σ_R (R^2 = 0.964).

Conclusion

Suzuki coupling of 5-bromo 9-hydroxyphenalenone with (hetero)aryl boronates efficiently furnishes an electronically diverse library of 5-(hetero)aryl substituted 9-HP derivatives, most remarkably dispensing the hydroxyl group protection. Almost all compounds display reversible reduction potentials, however, upon donor-substitution additionally irreversible oxidation waves can be identified. Absorption spectroscopy reveals three major absorption bands around 280, 360, and 450 nm for most derivatives as indicated by their yellow color. The longest wavelength maximum can be shifted to red and purple by positioning of moderately, and even more so, of strongly electron-donating groups. In addition all compounds fluoresce in solution with substantial quantum yields (up to 0.32). TD-DFT calculations nicely reproduce the experimental results of the absorption and emission spectroscopy and thereby rationalize the characteristics of the electronic structure. The concise, efficient synthesis gives access to a novel type of multifunctional chromophores possessing in addition to tunable absorption characteristics also emission and redox activity, as well as an additional special feature by chelating hydroxyl and carbonyl groups of the 9-HP acceptor moiety. Studies addressing the syntheses of further 9-HP derivatives and coordination compounds as well as investigations of the electronic properties are currently underway.

CCDC 1530859 (**3a**) and 1530860 (**3i**), respectively, contain the supplementary crystallographic data for this paper. These data are provided free of charge by The Cambridge Crystallographic Data Centre.

Experimental Section

Experimental Details

Typical procedure for the synthesis of 5-(hetero)aryl substituted 9-hydroxyphenalenone: In a Schlenk tube with magnetic stir bar under nitrogen atmosphere 5-bromo-9-hydroxy-1*H*-phenalen-1-one (**1**) (69 mg, 0.25 mmol, 1.00 equiv.) was dissolved in 1,4-dioxane (1.5 mL) and deionized water (0.5 mL). Tetrakis(triphenylphosphane)palladium(0) (29 mg, 10 mol%), $NaHCO_3$ (52 mg, 0.63 mmol, 2.5 equiv.) and the boronic acid (**2**) (0.28 mmol, 1.1 equiv.) were added and the reaction mixture was stirred at 100 °C (oil bath) for 18 h. After cooling to room temperature dichloromethane (5.0 mL), deionized water (10 mL) and conc. aqueous HCl (2.0 mL) were successively added. Then, the aqueous layer was extracted several times with dichloromethane (3×10 mL). The combined organic layers were dried (anhydrous magnesium sulfate), filtered, and the solvents were removed in vacuo. The crude products were recrystallized from acetonitrile and dried at 70 °C for 48 h under reduced pressure to give the desired 9-hydroxyphenalenone derivatives **3**.

Acknowledgements

We cordially thank the Volkswagen Stiftung (Az. 88 383-88 386), the Deutsche Forschungsgemeinschaft (Mu 1088/9-1), and the Fonds der Chemischen Industrie for financial support.

Computational support and infrastructure was provided by the "Centre for Information and Media Technology" (ZIM) at the University of Düsseldorf (Germany).

Conflict of interest

The authors declare no conflict of interest.

Keywords: cyclic voltammetry · density functional calculations · donor–acceptor systems · fluorescence · heterocycles

[1] a) T. J. J. Müller, in *Functional Organic Materials*, Wiley-VCH, **2007**, pp. 179 – 223; b) L. Levi, T. J. J. Müller, *Chem. Soc. Rev.* **2016**, *45*, 2825 – 2846.

[2] a) T. Meyer, D. Ogermann, A. Pankrath, K. Kleinermanns, T. J. J. Müller, *J. Org. Chem.* **2012**, *77*, 3704 – 3715; b) J. Mao, N. He, Z. Ning, Q. Zhang, F. Guo, L. Chen, W. Wu, J. Hua, H. Tian, *Angew. Chem.* **2012**, *124*, 10011 – 10014; c) M. Xu, R. Li, N. Pootrakulchote, D. Shi, J. Guo, Z. Yi, S. M. Zakeeruddin, M. Grätzel, P. Wang, *J. Phys. Chem. C* **2008**, *112*, 19770 – 19776.

[3] a) A. Harriman, *Angew. Chem. Int. Ed.* **2004**, *43*, 4985 – 4987; *Angew. Chem.* **2004**, *116*, 5093 – 5095; b) D. M. Arias-Rotondo, J. K. McCusker, *Chem. Soc. Rev.* **2016**, *45*, 5803 – 5820.

[4] a) S. Kim, S. Lee, T. F. Anjong, H. Y. Jang, J.-Y. Kim, C. Lee, S. Park, H. J. Lee, J. Yoon, J. Kim, *J. Phys. Chem. C* **2016**, *120*, 28407 – 28414; b) J. Fernández-Ariza, R. M. Krick Calderón, M. S. Rodríguez-Morgade, D. M. Guldi, T. Torres, *J. Am. Chem. Soc.* **2016**, *138*, 12963 – 12974; c) C. B. Kc, G. N. Lim, V. N. Nesterov, P. A. Karr, F. D'Souza, *Chem. Eur. J.* **2014**, *20*, 17100 – 17112.

[5] a) T.-S. Hsieh, J.-Y. Wu, C.-C. Chang, *Dyes Pigm.* **2015**, *112*, 34 – 41; b) S. Bay, T. Villnow, G. Ryseck, V. Rai-Constapel, P. Gilch, T. J. J. Müller, *ChemPlusChem* **2013**, *78*, 137 – 141.

[6] K. Arimitsu, R. Endo, *Chem. Mater.* **2013**, *25*, 4461 – 4463.

[7] H. Tian, X. Yang, R. Chen, Y. Pan, L. Li, A. Hagfeldt, L. Sun, *Chem. Commun.* **2007**, 3741 – 3743.

[8] a) S. K. Pal, M. E. Itkis, R. W. Reed, R. T. Oakley, A. W. Cordes, F. S. Tham, T. Siegrist, R. C. Haddon, *J. Am. Chem. Soc.* **2004**, *126*, 1478 – 1484; b) A. Pariyar, G. Vijaykumar, M. Bhunia, S. K. Dey, S. K. Singh, S. Kurungot, S. K. Mandal, *J. Am. Chem. Soc.* **2015**, *137*, 5955 – 5960.

[9] a) A. Das, T. M. Scherer, P. Mondal, S. M. Mobin, W. Kaim, G. K. Lahiri, *Chem. Eur. J.* **2012**, *18*, 14434 – 14443; b) S. K. Dey, A. Honecker, P. Mitra, S. K. Mandal, A. Mukherjee, *Eur. J. Inorg. Chem.* **2012**, *35*, 5814 – 5824; c) T. Mochida, R. Torigoe, T. Koinuma, C. Asano, T. Satou, K. Koike, T. Nikaido, *Eur. J. Inorg. Chem.* **2006**, *3*, 558 – 565; d) Y. Demura, T. Kawato, H. Kanatomi, I. Murase, *Bull. Chem. Soc. Jpn.* **1975**, *48*, 2820 – 2824; e) Y.-J. Gu, B. Yan, *Inorg. Chim. Acta* **2013**, *408*, 96 – 102.

[10] C. F. Koelsch, J. A. Anthes, *J. Org. Chem.* **1941**, *6*, 558 – 565.

[11] a) J. D. Loudon, R. K. Razdan, *J. Chem. Soc.* **1954**, 4299 – 4303; b) H. Silberman, S. Silberman, *Austral. J. Sci.* **1956**, *19*, 115; c) G. A. Reynolds, J. A. Van Allan, *J. Heterocycl. Chem.* **1969**, *6*, 375 – 377; d) G. Weeratunga, M. Austrup, R. Rodrigo, *J. Chem. Soc. Perkin Trans. 1* **1988**, 3169 – 3173; e) R. C. Haddon, F. Wudl, M. L. Kaplan, J. H. Marshall, R. E. Cais, F. B. Bramwell, *J. Am. Chem. Soc.* **1978**, *100*, 7629 – 7633.

[12] a) R. C. Haddon, S. V. Chichester, S. L. Mayo, *Synthesis* **1985**, *1985*, 639 – 641; b) X. Chi, M. E. Itkis, K. Kirschbaum, A. A. Pinkerton, R. T. Oakley, A. W. Cordes, R. C. Haddon, *J. Am. Chem. Soc.* **2001**, *123*, 4041 – 4048; c) X. Chi, M. E. Itkis, R. W. Reed, R. T. Oakley, A. W. Cordes, R. C. Haddon, *J. Phys. Chem. B* **2002**, *106*, 8278 – 8287; d) T. K. Sen, A. Mukherjee, A. Modak, P. K. Ghorai, D. Kratzert, M. Granitzka, D. Stalke, S. K. Mandal, *Chem. Eur. J.* **2012**, *18*, 54 – 58.

[13] a) A. Das, T. M. Scherer, S. M. Mobin, W. Kaim, G. K. Lahiri, *Inorg. Chem.* **2012**, *51*, 4390 – 4397; b) P. P. S. A. Mukherjee, C. Schulzke, S. K. Mandal, *J. Chem. Sci.* **2014**, *126*, 1581 – 1588.

[14] A. Das, T. K. Ghosh, A. Dutta Chowdhury, S. M. Mobin, G. K. Lahiri, *Polyhedron* **2013**, *52*, 1130 – 1137.

[15] S. K. Mandal, S. Samanta, M. E. Itkis, D. W. Jensen, R. W. Reed, R. T. Oakley, F. S. Tham, B. Donnadieu, R. C. Haddon, *J. Am. Chem. Soc.* **2006**, *128*, 1982 – 1994.

[16] G. He, Y. Hou, D. Sui, X. Wan, G. Long, P. Yun, A. Yu, M. Zhang, Y. Chen, *Tetrahedron* **2013**, *69*, 6890 – 6896.

[17] A. Kovács, V. Izvekov, K. Zauer, K. Ohta, *J. Phys. Chem. A* **2001**, *105*, 5000 – 5009.

[18] X.-J. Yang, F. Drepper, B. Wu, W.-H. Sun, W. Haehnel, C. Janiak, *Dalton Trans.* **2005**, 256 – 267.

[19] J. Shorter, *Chem. unserer Zeit* **1985**, *19*, 197 – 208.

[20] C. Hansch, A. Leo, R. W. Taft, *Chem. Rev.* **1991**, *91*, 165 – 195.

[21] N. Boens, W. Qin, N. Basarić, J. Hofkens, M. Ameloot, J. Pouget, J.-P. Lefèvre, B. Valeur, E. Gratton, M. vandeVen, N. D. Silva, Y. Engelborghs, K. Willaert, A. Sillen, G. Rumbles, D. Phillips, A. J. W. G. Visser, A. van Hoek, J. R. Lakowicz, H. Malak, I. Gryczynski, A. G. Szabo, D. T. Krajcarski, N. Tamai, A. Miura, *Anal. Chem.* **2007**, *79*, 2137 – 2149.

[22] R. Haddon, *Aust. J. Chem.* **1984**, *37*, 2145 – 2151.

[23] D. H. Ripin, D. A. Evans, evans.rc.fas.harvard.edu/pdf/evans_pKa_table.pdf **2005**.

[24] a) C. Lee, W. Yang, R. G. Parr, *Phys. Rev. B* **1988**, *37*, 785 – 789; b) A. D. Becke, *J. Chem. Phys.* **1993**, *98*, 1372 – 1377; c) K. Kim, K. D. Jordan, *J. Phys. Chem.* **1994**, *98*, 10089 – 10094; d) P. J. Stephens, F. J. Devlin, C. F. Chabalowski, M. J. Frisch, *J. Phys. Chem.* **1994**, *98*, 11623 – 11627.

[25] R. Krishnan, J. S. Binkley, R. Seeger, J. A. Pople, *J. Chem. Phys.* **1980**, *72*, 650 – 654.

[26] G. Scalmani, M. J. Frisch, *J. Chem. Phys.* **2010**, *132*, 114110.

Manuscript received: February 6, 2017
Accepted manuscript online: May 4, 2017
Version of record online: June 26, 2017

